Available online at www.sciencedirect.com
ScienceDirect
Journal of Solid State Chemistry 180 (2007) 3463–3468
JOURNAL OF SOLID STATE CHEMISTRY
www.elsevier.com/locate/jssc

Partial charge ordering in the mixed-valent compound $(Bi_6O_5)Rh_8^{3+}Rh_4^{4+}O_{24}$

H. Mizoguchi[a], W.J. Marshall[b], A.P. Ramirez[c], A.W. Sleight[a], M.A. Subramanian[a,*]

[a]Department of Chemistry and OSUMI, Oregon State University, Corvallis, OR 97331-4003, USA
[b]Central Research and Development, Dupont Company, Experimental Station, Wilmington, DE 19880-0228, USA
[c]Bell Laboratories, Alcatel-Lucent, 600 Mountain Avenue, Murray Hill, NJ 07974, USA

Received 9 August 2007; received in revised form 26 September 2007; accepted 27 September 2007
Available online 4 October 2007

Abstract

Crystals of the mixed-valent compound $(Bi_6O_5)Rh_8^{3+}Rh_4^{4+}O_{24}$ were grown from a flux. The room temperature conductivity of a crystal was 3 S/cm but decreased smoothly with decreasing temperature to 10^{-5} S/cm at 25 K. Magnetic susceptibility data indicate a localized moment for Rh^{4+}. A Seebeck coefficient at 200 K of $+280\,\mu V/K$ further confirms that this compound is a semiconductor rather than a metal with a partially filled 4d t_{2g} band. A structure refinement based on single crystal X-ray diffraction data obtained at 173 and 296 K provided Rh–O distances sufficiently accurate to indicate the nature of the charge ordering between Rh^{3+} and Rh^{4+}. The large Seebeck coefficient coupled with the high electrical conductivity indicates that this may be a promising low-temperature thermoelectric material.

Keywords: Rhodium oxide; Charge ordering; Bismuth; Electrical properties; Seebeck coefficient

1. Introduction

Preparation of rhodium oxide in air results in Rh_2O_3, and high pressure is required to obtain RhO_2 [1–4]. Likewise, high pressure is generally required to prepare ternary oxides of Rh^{4+} such as $BaRhO_3$, $SrRhO_3$, $Sr_4Rh_3O_{10}$, and $Sr_3Rh_2O_7$ [5–8]. However, Sr_2RhO_4 can be prepared in air and ternary oxides of Rh prepared in air are frequently mixed-valent Rh^{3+}/Rh^{4+} compounds. For example, $Ba_9Rh_8O_{24}$, $Ba_{11}Rh_{10}O_{30}$, $Ba_{32}Rh_{29}O_{87}$, $Ba_{1.72}Rh_8O_{16}$, $Ba_{1.21}Bi_{0.33}Rh_8O_{16}$, $Sr_{0.75}Rh_4O_8$, $Sr_6Rh_5O_{15}$, and $Ln_{18}Li_8Rh_5O_{39}$ where Ln can be La or Pr have been prepared in air [9–16]. This propensity of Rh to form Rh^{3+}/Rh^{4+} mixed oxides leads to formation of some rhodate structures analogous to those found for Mn^{3+}/Mn^{4+} and Ti^{3+}/Ti^{4+} oxides. For example, the Hollandite structure (Fig. 1a) is found for both $K_{1.33}Mn_8O_{16}$ and $(Ba,Cs)Ti_8O_{16}$, and it is also found for $Sr_{0.75}Rh_4O_8$, $Ba_{1.72}Rh_8O_{16}$, and $Ba_{1.21}Bi_{0.33}Rh_8O_{16}$ [17–19]. The Hollandite structure is based on a network of composition MO_2 where M octahedra share edges as in the rutile structure (Fig. 1). However in the case of the Hollandite structure, the connectivity produces channels that can contain large cations such as K^{1+}, Cs^{1+}, and Ba^{2+}. Much larger channels are found in another MO_2 network of octahedra in the case of the mineral Todorokite (Fig. 1c) [17]. Here the network cations are Mn^{3+}, Mn^{4+}, Al^{3+}, and Mg^{2+}, and the channels contain Ca^{2+}, Na^{1+}, K^{1+}, and H_2O. It is common for the contents of the channels of compounds with the Hollandite and Todorokite structures to be so disordered that their positions cannot be located by diffraction analysis. Very recently $[SrF_{0.8}(OH)_{0.2}]_{2.526}[Mn_6O_{12}]$ with the Todorokite structure was synthesized and found to have a well organized structure within the channels [20]. The compound $(Bi_6O_5)Rh_{12}O_{24}$ was also recently reported to have the same basic structure as Todorokite [21]. We report here on the physical properties of this compound and its structure based on single crystal X-ray diffraction data. Our interest is this compound relates to possible charge ordering in a mixed-valent system and the potential of this compound as a thermoelectric material.

*Corresponding author. Fax: +1 541 737 2062.
E-mail address: mas.subramanian@oregonstate.edu (M.A. Subramanian).

0022-4596/$ - see front matter © 2007 Elsevier Inc. All rights reserved.
doi:10.1016/j.jssc.2007.09.031

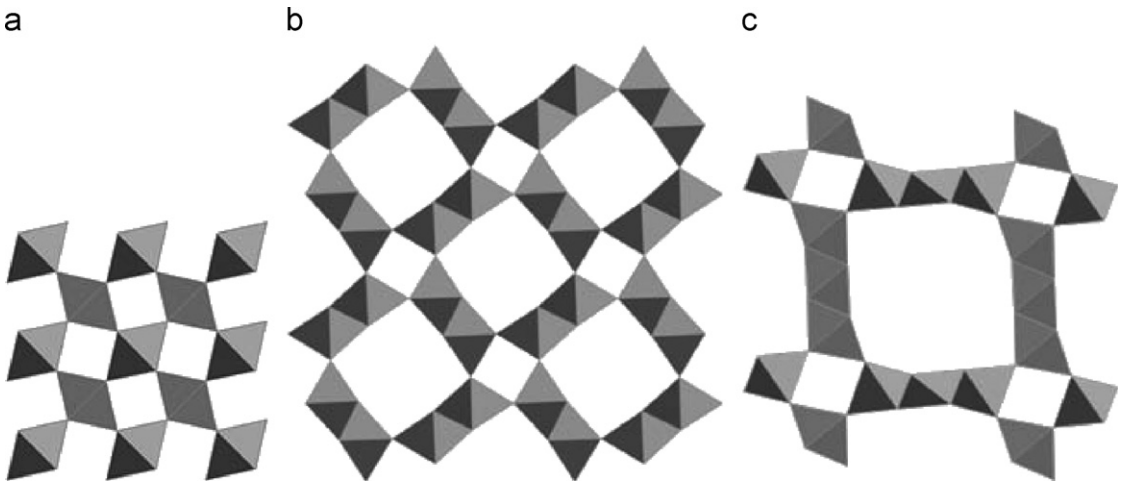

Fig. 1. The MO_2 networks in the structures of (a) rutile, (b) Hollandite, and (c) Todorokite. In all cases, the octahedra share edges to form chains in the third direction.

2. Experimental

Reactants were Bi_2O_3 (99.9%, Baker) and Rh_2O_3 prepared from $RhCl_3 \cdot xH_2O$ (99.9%, Alfa, Aesar) by heating in moist air at 1073 K for 10 h. Appropriate amounts of Bi_2O_3 and Rh_2O_3 were mixed by grinding together under ethanol in an agate mortar. This pressed mixture was placed in an alumina boat and heated in air at 1173 K for 30 h with two intermediate grindings. Heating to 1270 K resulted in the decomposition of $(Bi_6O_5)Rh_{12}O_{24}$ and the formation of Rh metal. Single crystals of $(Bi_6O_5)Rh_{12}O_{24}$ were grown in a flux of 90 wt% Bi_2O_3 and 10 wt% V_2O_5. An intimate mixture of polycrystalline $(Bi_6O_5)Rh_{12}O_{24}$ powder (0.3 g), Bi_2O_3 (5.4 g), V_2O_5 (0.6 g) was heated to 1420 K under air in a covered alumina crucible. After holding for 8 h, the crucible was cooled to 970 K at a rate of 3 K/h. After reaching 970 K, it was cooled to room temperature at a rate of 300 K/h. The flux was dissolved in HNO_3(aq) at 370 K. The product consisted of lustrous black needles several mm in length.

Single crystal X-ray diffraction data were collected on a Bruker SMART APEXII CCD system at both 173 and 296 K. A standard focus tube was used with an anode power of 50 kV at 30 mA, a crystal to plate distance of 5.0 cm, 512×512 pixels/frame, beam center (256.52, 253.16), total frames of 6602, oscillation/frame of 0.50°, exposure/frame of 10.0 s/frame, and SAINT integration. A subsequent SADABS correction was applied. The structures were refined by full-matrix least squares using shelxtl software. Further details are given in Table 1 and available cif files.

DC electrical conductivity measurements on a crystal were conducted by conventional four-probe methods over the temperature region 20–500 K. Seebeck coefficient measurements on a sintered pellet were conducted over the temperature region 170–500 K. The dc magnetization was measured with a conventional SQUID magnetometer from 2 to 300 K. EUTAX software was used to calculate bond valences.

Table 1
Crystallographic information for $Bi_6Rh_{12}O_{29}$

	173 K	296 K
Crystal size	$0.15 \times 0.03 \times 0.03$ mm	$0.15 \times 0.03 \times 0.03$ mm
Crystal system	Monoclinic	Monoclinic
Space group	$C2/m$	$C2/m$
a	19.833(1) Å	19.839(4) Å
b	12.224(1) Å	12.226(2) Å
c	9.5036(7) Å	9.516(2)
β	97.274(2)°	97.276(4)°
Volume	2285.4(3) Å^3	2289.5(7) Å^3
ρ_{calc}	8.582 g/cm^3	8.566 g/cm^3
$2\theta_{max}$	68.14°	68.30°
Wavelength (Mo)	0.71073 Å	0.71073 Å
Measured reflections	65501	73923
Unique reflections	4706	4732
μ(Mo)	54.54 mm^{-1}	54.54 mm^{-1}
h	+30 to −30	+31 to −31
k	+16 to −19	+10 to −18
l	+14 to −14	+14 to −14
R (int)	0.0727	0.0532
Parameters	232	222
Goodness of fit	1.06	1.09
$R(I>4\sigma(I))$	0.0271	0.0232
$wR(I>4\sigma(I))$	0.0598	0.0537
R(all data)	0.0341	0.0263
wR(all data)	0.0613	0.0546
Max difference peak	+4.55 e/Å^3	+3.657 e/Å^3
Max difference hole	−2.74 e/Å^3	−3.566 e/Å^3

3. Results

Our refined structure is essentially the same as that previously reported from X-ray powder diffraction data [21]. However, in that refinement only isotropic displacement factors were used with all 9 Rh atoms constrained to the same value and all 18 O atoms constrained to the same

value. The most significant difference between the refinements, however, is that our refinements provide much more accurate coordinates for the O atoms. This then produces much more accurate Rh–O distances for calculating Rh bond valence values.

The magnetic susceptibility for $(Bi_6O_5)Rh_{12}O_{24}$ is shown in Fig. 2. The data are fit well by the Curie–Weiss law yielding an effective high-temperature moment of $p_{eff} = 2.25\,\mu B$ per mole Rh^{4+} and an Weiss constant of -339 K. The value of p_{eff} is significantly greater than that expected for $S = 1/2$, presumably due to a large orbital contribution. The ordering at the inflection of $\chi(T)$ near 50 K is antiferromagnetic like. Thus we conclude that the magnetic order is essentially antiferromagnetic like among a subset of localized Rh moments. Finally, the upturn in $\chi(T)$ below 30 K is most likely due to unpaired Rh moments, in the density range of 1% of the Rh density.

The electrical resistivity of a $(Bi_6O_5)Rh_{12}O_{24}$ crystal was measured along the b-axis, and shows semiconducting-like behavior (Fig. 3). The data below 70 K can be fit by $\rho = A\exp(\Delta/T)$ with a single value of $\Delta = 20.3$ meV. No signature indicating charge order is seen near 50 K, suggesting that, if charge order occurs, it does not affect the primary conduction path. The Seebeck coefficient measured on a sintered pellet is shown in Fig. 4.

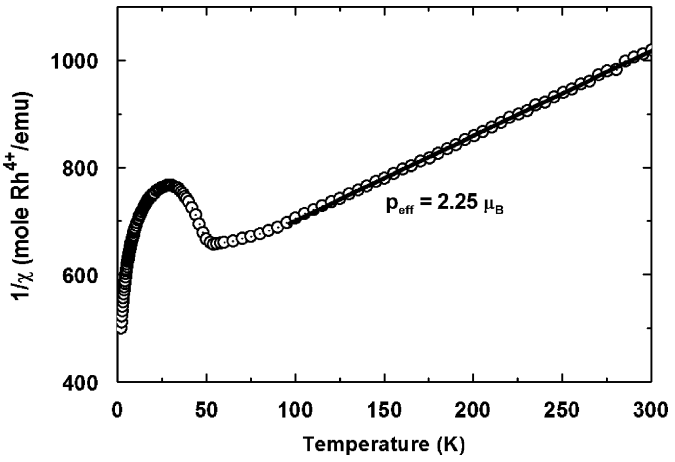

Fig. 2. The magnetic susceptibility vs. temperature for $(Bi_6O_5)Rh_{12}O_{24}$.

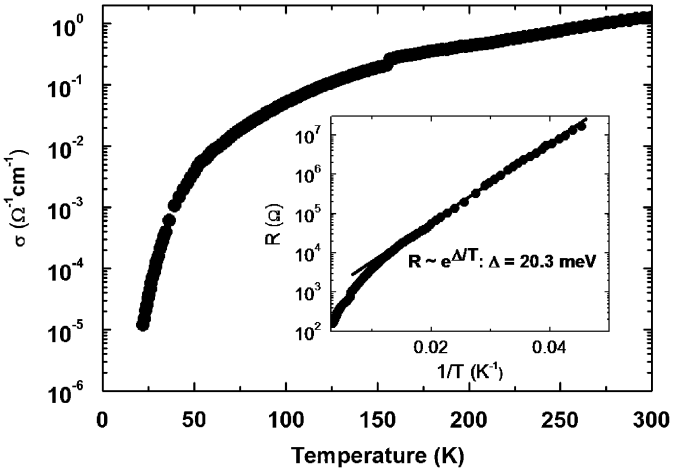

Fig. 3. The electrical conductivity vs. temperature for $(Bi_6O_5)Rh_{12}O_{24}$.

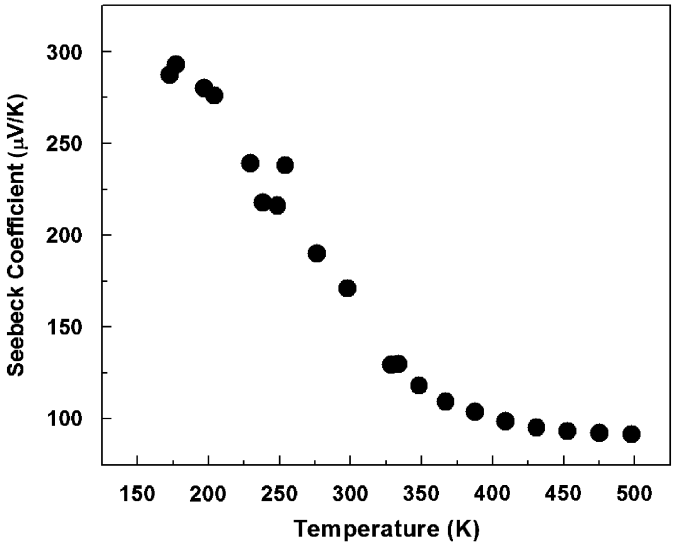

Fig. 4. The Seebeck coefficient vs. temperature for $(Bi_6O_5)Rh_{12}O_{24}$.

4. Discussion

The connectivity in the Todorokite structure is such that the highest possible symmetry would be tetragonal as is the case for the Hollandite structure (Fig. 1). The Hollandite structure is actually observed in both tetragonal and monoclinic symmetry. There is no intermediate orthorhombic version because there is no orthorhombic space group that is a subgroup of the tetragonal Hollandite space group. The mineral Todorokite has monoclinic symmetry as does $(Bi_6O_5)Rh_{12}O_{24}$ [22]. One measure of the distortion from tetragonal symmetry is the β angle, which is 93.7° in Todorokite and 97.3° in $(Bi_6O_5)Rh_{12}O_{24}$ [22]. Strong pseudotetragonal symmetry is observed in $[SrF_{0.8}(OH)_{0.2}]_{2.526}[Mn_6O_{12}]$ where the β angle is 90.2° [19]. The volume within the network channels shrinks as β deviates from 90°. Thus, we can say that the MO_2 network in $(Bi_6O_5)Rh_{12}O_{24}$ is more collapsed than in Todorokite and much more collapsed than in $[SrF_{0.8}(OH)_{0.2}]_{2.526}[Mn_6O_{12}]$. This large collapse for $(Bi_6O_5)Rh_{12}O_{24}$ is undoubtedly due to bonding between the RhO_2 network and the Bi_6O_5 chains. A major difference between the Todorokite and $(Bi_6O_5)Rh_{12}O_{24}$ structures is that the a-axis of $(Bi_6O_5)Rh_{12}O_{24}$ is increased by a factor of 2 and the b-axis by a factor of 4, relative to that of Todorokite. The increase in the b-axis is the result of structure of the Bi_6O_5 chain, which shows no semblance of a shorter repeat distance (Fig. 5). The doubling of the a-axis is the result of a shift along the b-axis of adjacent Bi_6O_5 chains. The Bi_6O_5 chain shown in Fig. 5 includes the Bi–O bonds to the RhO_2 network. The Bi–O bond distances involving network O are as short as 2.275 Å; thus, the Bi_6O_5 chains are very strongly bound to the RhO_2

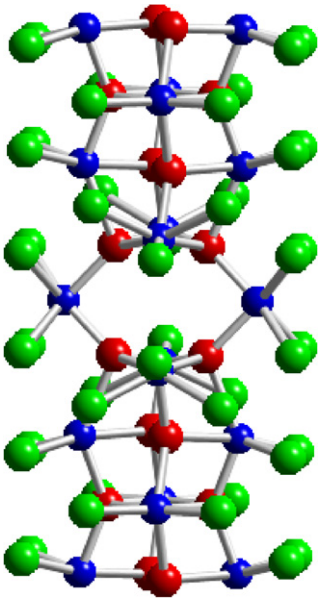

Fig. 5. The Bi_6O_5 chains where the Bi atoms are black (violet in on-line version); O atoms bound to Bi only are dark gray (red in on-line version) and O atoms bound also to Rh are light gray (green in on-line version).

network. The Bi–O polyhedra exhibit some edge sharing, which is common in other Bi–O chains [23,24]. The Bi atoms across the edge can be Bi1-Bi1, Bi1-Bi2, Bi2-Bi3, or Bi3-Bi3. The Bi4 atoms are not involved in edge sharing. There are always 2 Bi atoms at a given value of y along the b-axis, related to each other by a two-fold axis. These Bi_6O_5 chains may be considered as fragments of a distorted NaCl structure with an oxygen vacancy between Bi4 atoms.

In the tetragonal Hollandite structure, all octahedral sites are equivalent. In the ideal tetragonal Todorokite structure, which has apparently never been observed, there would be two types of octahedral sites. One octahedron shares two of its edges in the ac plane while the other octahedron shares only one of its edges in this plane (Fig. 1c). In the actual monoclinic structure of the mineral Todorokite, there are four crystallographically distinct octahedral sites. In $(Bi_6O_5)Rh_{12}O_{24}$ we have nine crystallographically distinct sites for Rh.

No Rh–Rh bonding is expected across the edge-shared octahedral in view of the filled or nearly filled 4 t_{2g} orbitals. This is confirmed by the Rh–Rh interatomic distances. For regular octahedra with an Rh–O distance of 2.02 Å, one would have O–O edge distances and Rh–Rh across edge distances of 2.86 Å. Instead the Rh–Rh distances across the edges have expanded to about 3.06 Å, and the O–O distance on these edges has contracted to about 2.75 Å.

Oxides of Rh^{3+} behave as classical semiconductors where the conduction band is a 4d e_g band, the valence band is a 4d t_{2g} band, and the band gap is about 2.2 eV. For oxides of Rh^{4+} the 4d t_{2g} band is 83% filled, and electrical conductivity measurements indicate itinerant electron behavior in RhO_2, $SrRhO_3$, $Sr_4Rh_3O_{10}$, $Sr_3Rh_2O_7$, and Sr_2RhO_4 [3,6–9]. One might then expect that $(Bi_6O_5)Rh_{12}O_{24}$ could be metallic with a 95% filled 4d t_{2g} band. Although $(Bi_6O_5)Rh_{12}O_{24}$ is a good electrical conductor, its conductivity is actually several orders of magnitude less than expected for a metal. Furthermore, its temperature dependence of conductivity is the opposite expected for a metal, and the high Seebeck coefficient is typical of a semiconductor rather than a metal. Finally, our magnetic susceptibility measurements show the presence of a localized moment. A similar temperature dependence of conductivity with a room temperature of 67 S/cm was observed for $Ba_{1.21}Bi_{0.33}Rh_8O_{16}$ with the Hollandite structure [13]. A room temperature conductivity of 0.1 S/cm was found for crystals of p-type $LuRhO_3$, and a room temperature conductivity of 0.7 S/cm was found for films of p-type $ZnRh_2O_4$ [25,26]. Because both of these materials were p-type, they may be regarded as a Rh^{3+}/Rh^{4+} mixed-valent compounds containing only a small amount of Rh^{4+}.

The previous report on $(Bi_6O_5)Rh_{12}O_{24}$ gave no information on physical properties [21]. Furthermore, the reported structure refinement based on X-ray powder diffraction data did not give atomic coordinates accurate enough to address the question of charge ordering related to the mixed valence of Rh^{3+}/Rh^{4+}. For example, bond valence calculations based on those reported coordinates give bond valences for Rh ranging from 2.98 to 4.33, which is outside the expected range. Bond valence calculations based on our coordinates from single crystal data give Rh valences ranging from 3.00 to 3.39 (Table 2 and Fig. 6). There are no significant changes in the Rh–O distances on cooling from room temperature to 173 K; thus, we can conclude that there is no change in the charge distribution over the various crystallographic site for Rh. Our bond valence calculations indicate that Rh5, Rh6, Rh7, and Rh9 are in the trivalent state. This is a reliable conclusion because the bond valence calculations for the Rh atoms were all based on the bond valence parameters established for Rh^{3+}. For the remainder of the Rh atoms, the bond valence for Rh is substantially above that expected for

Table 2
Rh interatomic distances and bond valences[a]

Atom	Rh–O (Å)	Bond valence
Rh7	2.048 (2.044)	3.00
Rh5	2.046 (2.044)	3.01
Rh6	2.038 (2.040)	3.03
Rh9	2.038 (2.036)	3.07
Rh1	2.018 (2.019)	3.28, *3.45*
Rh2	2.015 (2.016)	3.29, *3.46*
Rh8	2.009 (2.011)	3.34, *3.51*
Rh4	2.010 (2.010)	3.36, *3.53*
Rh3	2.005 (2.004)	3.39, *3.56*

[a]Average Rh–O distance for each Rh–O octahedron, which are accurate to ±0.002 Å based on standard deviations of individual Rh–O distances. Bond valences calculated with individual Rh–O distances, not their average. Values in parentheses are based on the refinement of data collected at 173 K. Values in italics are renormalized based on stoichiometry.

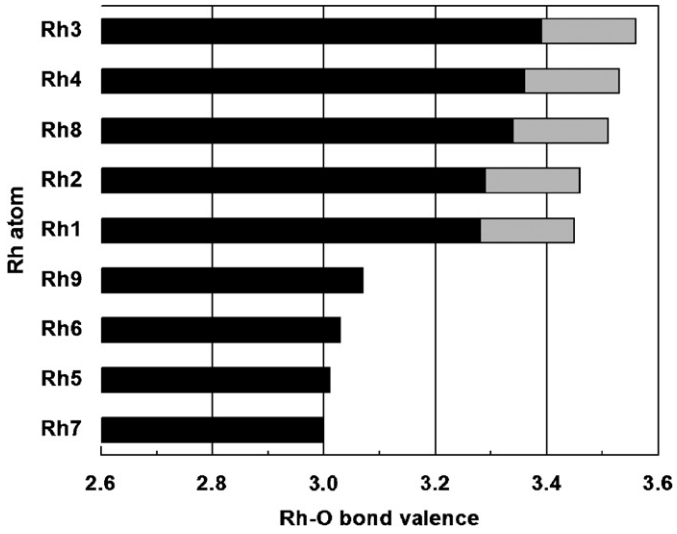

Fig. 6. The Rh bond valences for the 7 Rh atoms in $(Bi_6O_5)Rh_{12}O_{24}$. The extended bars for the top 5 Rh atoms are after renormalization based on stoichiometry.

Rh^{3+}. Thus, none of these sites can be occupied by Rh^{3+} only. The absolute values of these higher values actually have no meaning because these should be calculated assuming Rh^{4+} or some mixture of Rh^{4+} and Rh^{3+}. This is, however, not possible because good bond valence parameters for Rh^{4+} have not been established. This lack of bond valence parameters for Rh^{4+} does not impede our ability determine the charge ordering in $(Bi_6O_5)Rh_{12}O_{24}$. The coordination and interateratomic distances of Bi atoms indicates that they are all Bi^{3+}. The stoichiometry of $(Bi_6O_5)Rh_{12}O_{24}$ then dictates that the average valence of the Rh atoms showing a high bond valence must be 3.5. Renormalizing the high Rh bond valence values to this average then gives the values in italics in Table 2. The bond valence values for the high valent Rh range from 3.45 to 3.56, leading to the conclusion that Rh^{3+} and Rh^{4+} are present in essentially equal amounts over the Rh1, Rh2, Rh3, Rh4, and Rh8 sites. Thus, we conclude that the charge ordering in $(Bi_6O_5)Rh_{12}O_{24}$ has occurred according the different sites in the ideal Todorokite structure as indicated in Fig. 7. These two sites are distinctly different from one another. The site containing only Rh^{3+} shares six edges with other octahedral: two Rh^{3+} octahedra and four mixed-valent Rh octahedra. The octahedra of mixed-valent Rh share edges with only four other octahedra: two Rh^{3+} octahedra and two mixed-valent octahedra. This charge ordering is favored by electrostatic considerations because there is only the lower valent Rh in the site where there are six Rh–Rh repulsive interactions at about 3.05 Å across the octahedral edges. The octahedra with the higher valent Rh, and therefore higher Rh–Rh repulsive interactions, have only four of these Rh–Rh interactions. Thus instead of the formula $(Bi6O5)Rh83^+Rh_4^{4+}O_{24}$ we now have a structural formula of $(Bi_6O_5)Rh_4^{3+}Rh_8^{35+}O_{24}$. Apparently, $Ln_{18}Li_8Rh_5O_{39}$ where Ln can be La or Pr is the only other example of a

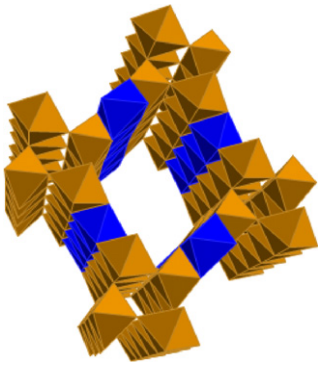

Fig. 7. The structure of $(Bi_6O_5)Rh_{12}O_{24}$ showing the chains of Rh^{3+} (black) (blue in on-line version) and $Rh^{3.5+}$ (gray) (gold in on-line version).

mixed-valent Rh compound where charge ordering has been established [16]. This conclusion was reached based on the different Rh–O distances for Rh^{3+} and Rh^{4+}.

The question remains as to why we lack structural evidence for complete charge ordering in $(Bi_6O_5)Rh_{12}O_{24}$. The part of the structure without apparent charge ordering is the same as the rutile structure (Figs. 1 and 7). This fragment contains edge-shared octahedra chains, and we might expect charge ordering based on simply alternating oxidation states along these chains. One answer for the lack of such order is that the space group for $(Bi_6O_5)Rh_{12}O_{24}$ does not allow such ordering. These chains in $(Bi_6O_5)Rh_{12}O_{24}$ are formed by Rh2 and Rh3 or by Rh1, Rh4, and Rh8. Actually, placing one oxidation state in the Rh1 site and the other in the Rh4 and Rh8 site does produce alternating Rh^{3+} and Rh^{4+} along some of the chains. However, ordering Rh^{3+} and Rh^{4+} in the Rh2 and Rh3 sites produces a chain of Rh^{3+}–Rh^{3+}–Rh^{4+}–Rh^{4+}–Rh^{3+}–Rh^{3+}, etc. Thus, a good scheme for charge ordering on these sites cannot be obtained with the constraint of $(Bi_6O_5)Rh_{12}O_{24}$ space group. But we are not constrained to this space group for charge ordering. Space groups normally change when charge ordering occurs. The real answer to the apparent lack of complete charge ordering can be understood by looking at ordering of cations in the rutile structure. There are many examples of $M^{3+}M^{5+}O_4$ compounds with the rutile structure [27]. No ordering of these cations has been observed for $CrTaO_4$, $FeTaO_4$, $RhTaO_4$, $CrNbO_4$, $FeNbO_4$, $RhNbO_4$, $AlSbO_4$, $CrSbO_4$, $FeSbO_4$, $RhSbO_4$, $GaSbO_4$, or $RhVO_4$. They may well be highly ordered in individual chains in one dimension, but three-dimensional order is frustrated. Cations in the rutile structure have two nearest neighbor cations in the chains and they have eight next nearest neighbors in adjacent chains. If there is alternating order within the chains, there is no way to order adjacent chains to obtain anything other than four neighbors of each kind. Thus, there is little impetus for three-dimensional order. Cation ordering is observed in $M^{3+}M^{5+}O_4$ compounds with the rutile structure when stabilized by metal–metal bonding of the M^{5+} cation as occurs in $CoReO_4$ and $AlWO_4$ or by metal–metal bonding of the M^{3+} cations as occurs in

$VSbO_4$ [28–31]. In these cases, each edge-shared chain is either all M^{3+} cations or all M^{5+} cations. This gives then closest near metal–metal neighbors of the same kind, but the all of the eight next near neighbors are of the opposite kind. Compounds of the type $M^{2+}M^{6+}O_4$ with octahedral cations usually do not form a rutile type structure. Typically, they have the wolframite structure with fully ordered cations. However, both $MgUO_4$ and $CuUO_4$ have rutile related structures [32,33]. With a formal charge difference of four, complete cation order is expected. These compounds overcome the frustration in different ways. The $MgUO_4$ structure is similar to that of $CoReO_4$ in that the edge-shared chains all contain Mg or U only. However, whereas the Co, Re, and Mg chains are all linear, the U chains are zigzagged such that U–U distances are slightly longer than Mg distances. Apparently, $CuUO_4$ is the only known rutile-type structure where different cations alternate along the edge-shared chains. The environment around Cu^{2+} is strongly distorted from octahedral with four Cu–O distances of about 1.95 Å and two Cu–O distances of 2.59 Å. More importantly, the eight metal–metal next nearest distances are now four like neighbors at 3.97 Å and four unlike neighbors at 3.69 Å, a very strong departure from the ideal rutile or orthorhombic $CoReO_4$ structures where all eight of these next nearest metal–metal distances are equal.

In conclusion, it is likely that complete charge ordering of Rh^{3+} and Rh^{4+} does occur with decreasing temperature in $(Bi_6O_5)Rh_{12}O_{24}$ in at least one dimension because only electron ordering is required, but our electrical conductivity data show no abrupt change that could be attributed to such charge ordering.

Acknowledgments

This work was supported by the Defense Advanced Research Projects Agency (MEMS/NEMS: Science and Technology Fundamentals) and Oregon Nanoscience and Microtechnology Institute (ONAMI).

Appendix A. Supplementary materials

Crystallographic data associated with this article can be obtained from the Fachinformationzentrum Karlsruhe, D-76344 Eggenstein-Leopoldshafen, Germany (Email: Crysdata@fiz-karlsruhe.de) on quoting depository numbers CSD 418623 and 418624.

References

[1] J.M.D. Coey, Acta Crystallogr. 26 (1970) 1876.
[2] J.W.M. Biesterbos, J.J. Hornstra, Less-Common Met. 30 (1973) 121.
[3] R.D. Shannon, Solid State Commun. 6 (1968) 139.
[4] O. Muller, R. Roy, J. Less-Common Met. 16 (1968) 129.
[5] B.L. Chamberland, J.B. Anderson, J. Solid State Chem. 39 (1981) 114.
[6] K. Yamaura, E. Takayama-Muromachi, Phys. Rev. B 64 (2001) 224424.
[7] K. Yamaura, Q. Huang, D.P. Young, E. Takayama-Muromachi, Chem. Mater. 16 (2004) 3424.
[8] K. Yamaura, Q. Huang, D.P. Young, Y. Noguchi, E. Takayama-Muromachi, Phys. Rev. B 66 (2002) 134431.
[9] T. Shimura, M. Itoh, T. Nakamura, J. Solid State Chem. 98 (1992) 198.
[10] K.E. Stitzer, M.D. Smith, J. Darriet, H.-C. zur Loye, Chem. Commun. (2001) 1680.
[11] K.E. Stitzer, E.A. Ahmed, J. Darriet, H.-C. zur Loye, J. Am. Chem. Soc. 126 (2004) 856.
[12] T. Siegrist, E.M. Larson, B.L. Chamberland, J. Alloys Compds. 210 (1994) 13.
[13] T. Klimczuk, W.-L. Lee, H.W. Zandbergen, R.J. Cava, Mater. Res. Bull. 39 (2004) 1671.
[14] J.R. Plaisier, A.A.C. van Vliet, D.J.W. Ijdo, J. Alloys Compds. 314 (2001) 56.
[15] J.B. Claridge, H.-C. zur Loye, Chem. Mater. 10 (1998) 2320.
[16] P.P.C. Frampton, P.D. Battle, C. Ritter, Inorg. Chem. 44 (2005) 7138.
[17] J.E. Post, Proc. Natl. Acad. Sci. USA 96 (1999) 3447.
[18] J. Vicat, E. Fanchon, P. Strobel, Q. Duc Tran, Acta Crystallogr. B 42 (1986) 162.
[19] R.W. Cheary, Acta Crystallogr. B 47 (1991) 325.
[20] A.M. Abakumov, J. Hadermann, G.V. Tendeloo, M.L. Kovba, Y.Y. Skolis, S.V. Mudretsova, E.V. Antipov, O.S. Volkova, A.N. Vasiliev, N. Tristan, R. Klingeler, B. Buchner, Chem. Mater. 19 (2007) 1181.
[21] F. Stowasser, C. Renkenberger, Z. Krist. 221 (2006) 206.
[22] J.E. Post, D.L. Bish, Am. Mineral. 73 (1988) 861.
[23] W. Wong-Ng, R.S. Roth, C.J. Rawn, J. Am. Ceram. Soc. 80 (1997) 324.
[24] I. Radosavljevic, J.A.K. Howard, A.W. Sleight, Int. J. Inorg. Mater. 2 (2000) 543.
[25] H.S. Jarrett, A.W. Sleight, H.H. Kung, J.L. Gilson, J. Appl. Phys. 51 (1980) 3916.
[26] H. Mizoguchi, M. Hirano, S. Fujitsu, T. Takeuchi, K. Ueda, H. Hosono, Appl. Phys. Lett. 80 (2002) 1207.
[27] A.F. Wells, Structural Inorganic Chemistry, Clarendon Press, Oxford, 1984.
[28] A.W. Sleight, Inorg. Chem. 14 (1974) 597.
[29] W.H. Baur, W. Joswig, G. Pieper, D. Kassner, J. Solid State Chem. 99 (1992) 207.
[30] T. Birchall, A.W. Sleight, Inorg. Chem. 15 (1976) 868.
[31] W.H. Baur, Zeit. Krist. 209 (1994) 143.
[32] W.H. Zachariasen, Acta Crystallogr. 7 (1954) 788.
[33] S. Siegel, H.R. Hoekstra, Acta Crystallogr. B 24 (1968) 967.